

TITLE

Ilia Kohanovski^a, Uri Obolski^{b,c}, and Yoav Ram^{a,*}

^aSchool of Computer Science, Interdisciplinary Center Herzliya, Herzliya 4610101, Israel

^bSchool of Public Health, Tel Aviv University, Tel Aviv 6997801, Israel

^cPorter School of the Environment and Earth Sciences, Tel Aviv University, Tel Aviv 6997801, Israel

*Corresponding author: yoav@yoavram.com

May 6, 2020

Abstract

Lorem ipsum dolor sit amet, consectetur adipiscing elit. Ut purus elit, vestibulum ut, placerat ac, adipiscing vitae, felis. Curabitur dictum gravida mauris. Nam arcu libero, nonummy eget, consectetur id, vulputate a, magna. Donec vehicula augue eu neque. Pellentesque habitant morbi tristique senectus et netus et malesuada fames ac turpis egestas. Mauris ut leo. Cras viverra metus rhoncus sem. Nulla et lectus vestibulum urna fringilla ultrices. Phasellus eu tellus sit amet tortor gravida placerat. Integer sapien est, iaculis in, pretium quis, viverra ac, nunc. Praesent eget sem vel leo ultrices bibendum. Aenean faucibus. Morbi dolor nulla, malesuada eu, pulvinar at, mollis ac, nulla. Curabitur auctor semper nulla. Donec varius orci eget risus. Duis nibh mi, congue eu, accumsan eleifend, sagittis quis, diam. Duis eget orci sit amet orci dignissim rutrum.

18 Introduction

19 The COVID-19 pandemic has resulted in implementation of extreme non-pharmaceutical interventions
20 (NPIs) in many affected countries. These interventions, from social distancing to lockdowns, are
21 applied in a rapid and widespread fashion. The NPIs are designed and assessed using epidemiological
22 models, which follow the dynamics of the viral infection to forecast the effect of different mitigation and
23 suppression strategies on the levels of infection, hospitalization, and fatality. These epidemiological
24 models usually assume that the effect of NPIs on disease transmission begins at the officially declared
25 date (e.g. Flaxman et al.⁵, Gatto et al.⁷, Li et al.⁹).

26 Adoption of public health recommendations is often critical for effective response to infectious dis-
27 eases, and has been studied in the context of HIV⁸ and vaccination^{3,12}, for example. However,
28 behavioral and social change does not occur immediately, but rather requires time to diffuse in the
29 population through media, social networks, and social interactions. Moreover, compliance to NPIs
30 may differ between different interventions and between people. For example, in a survey of 2,108
31 adults in the UK during Mar 2020, Atchison et al.² found that those over 70 years old were more likely
32 to adopt social distancing than young adults (18-34 years old), and that those with lower income were
33 less likely to be able to work from home and to self-isolate. Furthermore, compliance to NPIs may be
34 impacted by risk perception, as perceived by the number of domestic cases or even by reported cases in
35 other regions and countries. Interestingly, the perceived risk of COVID-19 infection has likely caused
36 a reduction in the number of influenza-like illness cases in the US starting from mid-February¹³.

37 Here, we hypothesize that there is a significant difference between the official start of NPIs and their
38 adoption by the public and therefore their effect on transmission dynamics. We use a *Susceptible-*
39 *Exposed-Infected-Recovered* (SEIR) epidemiological model and *Markov Chain Monte Carlo* (MCMC)
40 parameter estimation framework to estimate the effective start date of NPIs from publicly available
41 COVID-19 case data in several geographical regions. We compare these estimates to the official
42 dates and find both delayed and advanced effect of NPIs on COVID-19 transmission dynamics. We
43 conclude by demonstrating how differences between the official and effective start of NPIs can confuse
44 assessments of the effectiveness of the NPIs in a simple epidemic control framework.

45 Models and Methods

46 **Data.** We use daily confirmed case data $\mathbf{X} = (X_1, \dots, X_T)$ from several different countries. These
47 incidence data summarize the number of individuals X_t tested positive for SARS-CoV-2 RNA (using
48 RT-qPCR) at each day t . Data for Wuhan, China retrieved from Pei and Shaman¹⁰, data for 11
49 European countries retrieved from Flaxman et al.⁵. Regions in which there were multiple sequences
50 of days with zero confirmed cases (e.g. France), we cropped the data to begin with the last sequence
51 so that our analysis focuses on the first sustained outbreak rather than isolated imported cases. For
52 dates of official NPI dates see Table 1.

53 **SEIR model.** We model SARS-CoV-2 infection dynamics by following the number of susceptible
54 S , exposed E , reported infected I_r , and unreported infected I_u individuals in a population of size N .
55 This model distinguishes between reported and unreported infected individuals: the reported infected
56 are those that have enough symptoms to eventually be tested and thus appear in daily case reports, to
57 which we fit the model.

58 Susceptible (S) individuals become exposed due to contact with reported or unreported infected
59 individuals (I_r or I_u) at a rate β_r or $\mu\beta_r$. The parameter $0 < \mu < 1$ represents the decreased transmission
60 rate from unreported infected individuals, who are often subclinical or even asymptomatic. The

Country	First	Last
Austria	Mar 10 2020	Mar 16 2020
Belgium	Mar 12 2020	Mar 18 2020
Denmark	Mar 12 2020	Mar 18 2020
France	Mar 13 2020	Mar 17 2020
Germany	Mar 12 2020	Mar 22 2020
Italy	Mar 5 2020	Mar 11 2020
Norway	Mar 12 2020	Mar 24 2020
Spain	Mar 9 2020	Mar 14 2020
Sweden	Mar 12 2020	Mar 18 2020
Switzerland	Mar 13 2020	Mar 20 2020
United Kingdom	Mar 16 2020	Mar 24 2020
Wuhan	Jan 23 2020	Jan 23 2020

Table 1: Official start of non-pharmaceutical interventions. The date of the first intervention is for a ban of public events, or encouragement of social distancing, or for school closures. In all countries except Sweden, the date of the last intervention is for a lockdown. In Sweden, where a lockdown was not ordered during the studied dates, the last date is for school closures. Dates for European countries from Flaxman et al.⁵, date for Wuhan, China from Pei and Shaman¹⁰.

transmission rate $\beta_t \geq 0$ may change over time t due to behavioural changes of both susceptible and infected individuals. Exposed individuals, after an average incubation period of Z days, become reported infected with probability α_t or unreported infected with probability $(1 - \alpha_t)$. The reporting rate $0 < \alpha_t < 1$ may also change over time due to changes in human behavior. Infected individuals remain infectious for an average period of D days, after which they either recover, or becomes ill enough to be quarantined. They therefore no longer infect other individuals, and the model does not track their frequency. The model is described by the following equations:

$$\begin{aligned}
\frac{dS}{dt} &= -\beta_t S \frac{I_p}{N} - \mu \beta_t S \frac{I_s}{N} \\
\frac{dE}{dt} &= \beta_t S \frac{I_p}{N} + \mu \beta_t S \frac{I_s}{N} - \frac{E}{Z} \\
\frac{dI_r}{dt} &= \alpha_t \frac{E}{Z} - \frac{I_r}{D} \\
\frac{dI_u}{dt} &= (1 - \alpha_t) \frac{E}{Z} - \frac{I_r}{D}.
\end{aligned} \tag{1}$$

The initial numbers of exposed $E(0)$ and unreported infected $I_u(0)$ are considered model parameters, whereas the initial number of reported infected is assumed to be zero $I_r(0) = 0$, and the number of susceptible is $S(0) = N - E(0) - I_u(0)$. This model is inspired by Li et al.⁹ and Pei and Shaman¹⁰, who used a similar model with multiple regions and constant transmission β and reporting rate α to infer COVID-19 dynamics in China and the continental US, respectively.

Likelihood function. The *expected* cumulative number of reported infected individuals until day t is

$$Y_t = \int_0^t \alpha_s \frac{E(s)}{Z} ds, \quad Y_0 = 0. \tag{2}$$

We assume that reported infected individuals are confirmed and therefore observed in the daily case report of day t with probability p_t (note that an individual can only be observed once, and that p_t may change over time, but t is a specific date rather than the time elapsed since the individual was infected).

Hence, we assume that the number of confirmed cases in day t is binomially distributed,

$$X_t \sim \text{Bin}(n_t, p_t),$$

where n_t is the *realized* (rather than expected) number of reported infected individuals yet to appear in daily reports by day t . The cumulative number of confirmed cases until day t is

$$\tilde{X}_t = \sum_{i=1}^t X_i, \quad X_0 = 0.$$

Given \tilde{X}_{t-1} , we assume n_t is Poisson distributed,

$$(n_t \mid \tilde{X}_{t-1}) \sim \text{Poi}(Y_t - \tilde{X}_{t-1}), \quad n_1 \sim \text{Poi}(Y_1).$$

77 Therefore, $(X_t \mid \tilde{X}_{t-1})$ is a binomial conditioned on a Poisson, which reduces to a Poisson with

$$78 \quad (X_t \mid \tilde{X}_{t-1}) \sim \text{Poi}\left((Y_t - \tilde{X}_{t-1}) \cdot p_t\right), \quad X_1 \sim \text{Poi}(Y_1 \cdot p_1). \quad (3)$$

79 For given vector θ of model parameters (Eq. (6)), we compute the expected cumulative number
80 of reported infected individuals $\{Y_t\}_{t=1}^T$ for each day (Eq. (2)). Then, since \tilde{X}_{t-1} is a function of
81 X_1, \dots, X_{t-1} , we can use Eq. (3) to write the probability to observe the confirmed case data $\mathbf{X} =$
82 (X_1, \dots, X_T) as

$$83 \quad \mathbb{L}(\theta \mid \mathbf{X}) = P(\mathbf{X} \mid \theta) = P(X_1 \mid \theta)P(X_2 \mid \tilde{X}_1, \theta) \cdots P(X_T \mid \tilde{X}_{T-1}, \theta). \quad (4)$$

84 This defines a *likelihood function* $\mathbb{L}(\theta \mid \mathbf{X})$ for the parameter vector θ given the data \mathbf{X} .

85 **NPI model.** To model non-pharmaceutical interventions (NPIs), we set the beginning of the NPIs
86 to day τ and define

$$87 \quad \beta_t = \begin{cases} \beta, & t < \tau \\ \beta\lambda, & t \geq \tau \end{cases}, \quad \alpha_t = \begin{cases} \alpha_1, & t < \tau \\ \alpha_2, & t \geq \tau \end{cases}, \quad p_t = \begin{cases} 1/9, & t < \tau \\ 1/6, & t \geq \tau \end{cases}, \quad (5)$$

88 where $0 < \lambda < 1$. The values for p_t follow Li et al.⁹, who estimated the average time between infection
89 and reporting in Wuhan, China, at 9 days before the start of NPIs (Jan 23, 2020) and 6 days after start
90 of NPIs. The parameter τ is then added to the parameter vector θ (Eq. (6)).

91 **Parameter estimation.** To estimate the parameters of our model from the data \mathbf{X} , we apply a
92 Bayesian inference approach. We start our model Δt days before the outbreak (defined as consecutive
93 days with increasing confirmed cases) in each country⁷. The model in Eq. (1) is parameterized by the
94 vector θ , where

$$95 \quad \theta = \left(Z, D, \mu, \{\beta_t\}, \{\alpha_t\}, \{p_t\}, E(0), I_u(0) \right), \tau, \Delta t. \quad (6)$$

96 The likelihood function is defined in Eq. (4). The posterior distribution of the model parameters
97 $P(\theta \mid \mathbf{X})$ is then estimated using an *affine-invariant ensemble sampler for Markov chain Monte Carlo*
98 (MCMC) implemented in the *emcee* Python package⁶.

99 We define the following priors on the model parameters $P(\theta)$:

$$\begin{aligned}
Z &\sim \text{Uniform}(2, 5) \\
D &\sim \text{Uniform}(2, 5) \\
\mu &\sim \text{Uniform}(0.2, 1) \\
\beta &\sim \text{Uniform}(0.8, 1.5) \\
\lambda &\sim \text{Uniform}(0, 1) \\
\alpha_1, \alpha_2 &\sim \text{Uniform}(0.02, 1) \\
E(0) &\sim \text{Uniform}(0, 3000) \\
I_u(0) &\sim \text{Uniform}(0, 3000) \\
\tau &\sim \text{TruncatedNormal}(\tau^*, 5, 1, T - 2),
\end{aligned} \tag{7}$$

101 where $\text{TruncatedNormal}(\mu, \sigma, a, b)$ is a truncated normal distribution with mean μ and standard deviation σ taking values between a and b ; T is the number of days in the data \mathbf{X} ; and τ^* is the official
102 start of the NPI. Most priors follow Li et al.⁹, with the following exceptions. λ is used to ensure
103 transmission rates are lower after the start of the NPIs ($\lambda < 1$). We checked values of Δt larger than
104 five days and found they generally produce lower likelihood and unreasonable parameter estimates.
105 For the effective start of NPIs τ we have also tested an uninformative uniform prior $U(1, T - 1)$. DIC
106 (see definition below) was lower for the truncated normal prior in most countries, except **Germany?**.
107 More importantly, the uninformative prior could result in non-negligible posterior probability for
108 unreasonable τ values, such as Mar 1 in the United Kingdom (this was due to MCMC chains being
109 stuck on values far from the MAP). We therefore decided to use the more informative truncated normal
110 prior.
111

112 **Model selection.** We perform model selection using DIC (deviance information criterion)¹¹,

$$\begin{aligned}
DIC(\theta, \mathbf{X}) &= 2\mathbb{E}[D(\theta)] - D(\mathbb{E}[\theta]) \\
&= 2\log \mathcal{L}(\mathbb{E}[\theta] | \mathbf{X}) - 4\mathbb{E}[\log \mathcal{L}(\theta | \mathbf{X})],
\end{aligned} \tag{8}$$

114 where $D(\theta) = -2\log \mathcal{L}(\theta | \mathbf{X})$ is the Bayesian deviance, and expectations $\mathbb{E}[\cdot]$ are taken over the pos-
115 terior distribution $P(\theta | \mathbf{X})$. We compare models by reporting their relative DIC; lower is better.

116 **Source code.** We use Python 3 (Anaconda) with the NumPy, Matplotlib, SciPy, Pandas, Seaborn,
117 and emcee packages. All source code will be publicly available under a permissive open-source
118 license at github.com/yoavram-lab/EffectiveNPI.

119 Results

120 Several studies have described the effects of non-pharmaceutical interventions in different geographical
121 regions^{5,7,9}. These studies have assumed that the parameters of the epidemiological model change at a
122 specific date, as in Eq. (5), and set the change date τ to the official NPI date τ^* (Table 1). They then fit
123 the model once for time $t < \tau^*$ and once for time $t \geq \tau^*$. For example, Li et al.⁹ estimate the dynamics
124 in China before and after τ^* at Jan 23. Thereby, they effectively estimate (β, α_1) and (λ, α_2) separately.
125 Here we estimate the posterior distribution $P(\tau | \mathbf{X})$ of the *effective* start date of the NPIs by jointly
126 estimating $\tau, \beta, \lambda, \alpha_1, \alpha_2$ on the entire data per region (e.g. Italy, Austria), rather than splitting the data
127 at τ^* . We then compute the maximum a posteriori estimate $\hat{\tau} = \text{argmax}_{\tau} P(\tau | \mathbf{X})$.

128 We find that a model that considers an NPI (Eq. (5)) is a better fit to the data than a model without an
129 NPI, i.e. with constant β and α (**$\Delta DIC > ?$ for all regions**.) We compare the official τ^* and effective $\hat{\tau}$

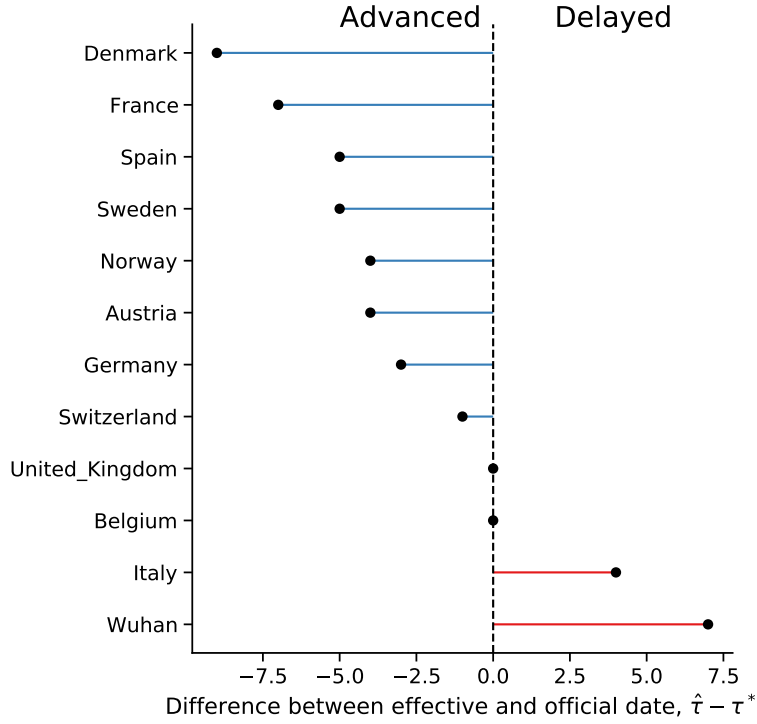


Figure 1: Official and effective start of non-pharmaceutical interventions.

130 start of NPIs and find that in most regions the effective start of NPI significantly differs from the official
 131 date (Figure 1): the 95% confidence interval on $\hat{\tau}$ does not include τ^* , and the DIC of the model with
 132 free τ parameter is lower than that of a model with a fixed $\tau \equiv \tau^*$ ($\Delta DIC > ?$.) The exception that
 133 proves the rule is Switzerland. We also find that the posterior distributions of τ are either unimodal
 134 (e.g. Italy) or flat (e.g. Sweden). The exception is the posterior of the United Kingdom, which
 135 has

136 In the following, we describe our findings on delayed and advanced start of NPI in detail.

137 **Delayed effective start of NPI.** In both Wuhan, China, and in Italy we find that our estimated
 138 effective start of NPI $\hat{\tau}$ is significantly later than the official date τ^* (Figure 1).

139 In Italy, the first case officially confirmed on Feb 21, a lockdown was declared in Northern Italy on
 140 Mar 8, with social distancing implemented in the rest of the country, and the lockdown was extended
 141 to the entire nation on Mar 11⁷. That is, the official date τ^* is either Mar 8 or 11. However, we
 142 estimate the effective date $\hat{\tau}$ at Mar 16 (± 0.7 days 95% CI ; Figure 2). Similarly, in Wuhan, China, a
 143 lockdown was ordered on Jan 23⁹, but we estimate the effective start of NPIs to be several days later
 144 at around Mar 2 (± 2.65 days 95% CI Figure 2).

145 **Advanced effective start of NPIs.** In contrast, in some regions we estimate an effective start of NPIs
 146 $\hat{\tau}$ that is *earlier* than the official date τ^* (Figure 1). In Spain, social distancing was encouraged starting
 147 on Mar 8⁵, but mass gatherings still occurred on Mar 8, including a march of 120,000 people for the
 148 International Women's Day, and a football match between Real Betis and Real Madrid (2:1) with a
 149 crowd of 50,965 in Seville. A national lockdown was only announced on Mar 14⁵. Nevertheless, we
 150 estimate the effective start of NPI $\hat{\tau}$ at Mar 8 or 9 (± 2.96 95%CI), rather than Mar 14 (Figure 3).

151 Similarly, in France the official lockdown started at Mar 17 (τ^*), with initial NPIs at Mar 13⁵.

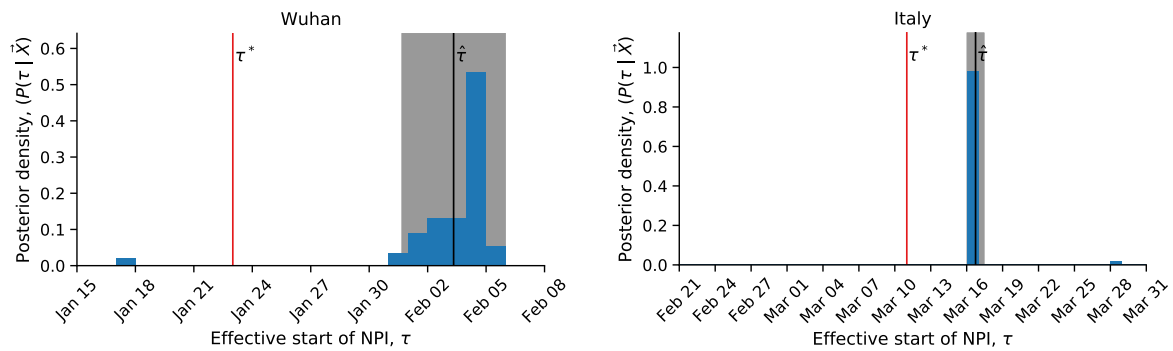


Figure 2: Delayed effect of non-pharmaceutical interventions in Italy and Wuhan, China.

152 However, we estimate the effective start of NPIs $\hat{\tau}$ at Mar 8 (± 5.9 days 95% CI). Although the
 153 confidence interval is wide, spanning from Mar 2 to Mar 13, the official lockdown start at Mar 17 is
 154 later still (Figure 3).

155 Interestingly, the effective start of NPIs $\hat{\tau}$ in both France and Spain is estimated at Mar 8, although
 156 the official dates are differ by three days. Moreover, the number of daily cases was similar until
 157 Mar 8 in both countries, but diverged by Mar 13, reaching significantly higher numbers in Spain
 158 (Figure S1).

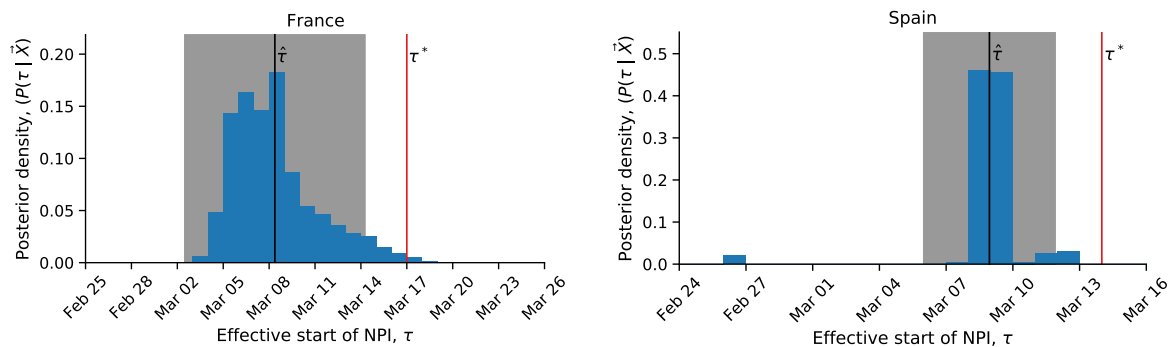


Figure 3: Advanced effect of non-pharmaceutical interventions in France and Spain. Posterior distribution of τ , the effective start date of NPI, is shown as a histogram of MCMC samples. Red line shows the official NPI date τ^* . Black line shows the MAP estimate $\hat{\tau}$. Shaded area shows a 95% confidence interval (area in which $P(|\tau - \hat{\tau}| | \mathbf{X}) = 0.95$).

159 **The exception that proves the rule.** We find one case in which the official and effective dates
 160 match: Switzerland ordered a national lockdown on Mar 20, after banning public evens and closing
 161 schools on Mar 13 and 14⁵. Indeed, our MAP estimate $\hat{\tau}$ is Mar 20, and the posterior distribution
 162 shows two density peaks: a smaller one between Mar 10 and Mar 14, and a taller one between Mar 17
 163 and Mar 22. It's also worth mentioning that Switzerland was the first to mandate self isolation of
 164 confirmed cases⁵.

165 **Effect of delays and advances of real-time assessment.** The success of non-pharmaceutical inter-
 166 ventions is assessed by health officials using various metrics, such as the decline in the growth rate
 167 of daily cases. These assessments are made a specific number of days after the intervention began,
 168 to accommodate for the expected serial interval (i.e. time between successive cases in a chain of
 169 transmission), which is estimated at about 4-7 days⁷.

170 However, a significant difference between the beginning of the intervention and the effective change
 171 in transmission rates can invalidate assessments that assume a serial interval of 4-7 days and neglect
 172 the delayed or advanced population response to the NPI. Such a case is illustrated in Figure 4 using
 173 data and parameters from Italy. Here, a lockdown is officially ordered on Mar 10 (τ^*), but its delayed
 174 effect on the transmission dynamics starts on Mar 15 ($\hat{\tau}$). If health officials assume the dynamics to
 175 immediately change at τ^* , they will expect the number of cases to follow the dashed red line. However,
 176 the number of cases will actually follow the black line, leading to a significant different (Δ) between
 177 the projections and the realization.

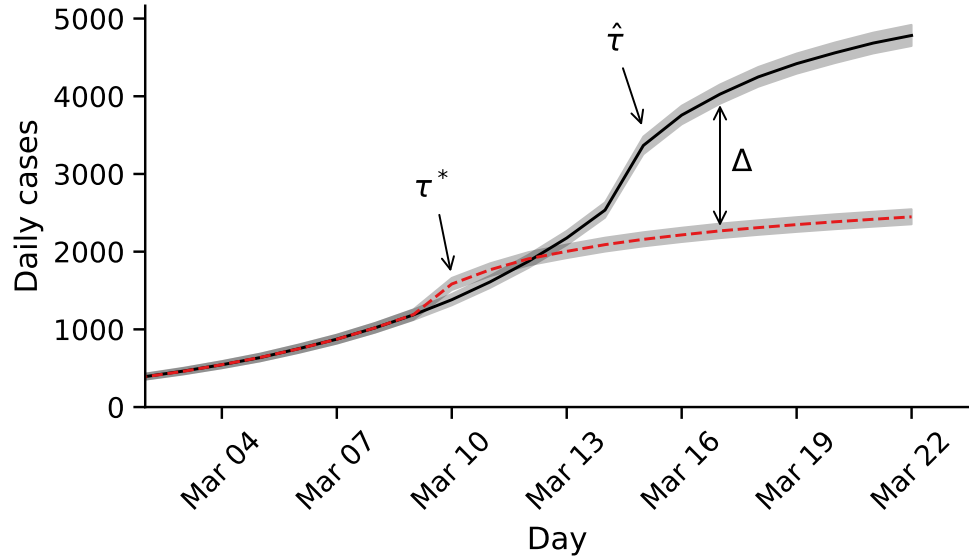


Figure 4: Delayed effective start of NPI causes leads to under-estimation of daily confirmed cases. The red and black lines show model predictions when NPIs start on the official date τ^* or on the effective date $\hat{\tau}$, respectively, with 95% confidence intervals. This demonstrates Δ the assessment error seven days after the official start of NPIs, which in this case is about 40%. Parameters are MAP estimates for Italy ([TABLE](#)).

178 Discussion

179 We have estimated the effective start date of NPIs in several geographical regions using an SEIR
180 epidemiological model and an MCMC parameter estimation framework. We find examples of both
181 advanced and delayed response to NPIs (Figure 1).

182 For example, in Italy and Wuhan, China, the effective start of the lockdowns seems to have occurred
183 3-5 after the official date (Figure 2). This could be explained by low compliance. In Italy, for example,
184 a leak about the intent to lockdown Northern provinces results in people leaving those provinces⁷.
185 However, delayed effect of NPIs could also be due to the time required by both the government and
186 the citizens to organize for a lockdown.

187 In contrast, in most investigated countries, such as Spain and France, transmission rates seem to
188 have been reduced even before official lockdowns were implemented (Figure 3). This advanced
189 response is possibly due to adoption of social distancing and similar behavioral adaptations in parts
190 of the population, maybe in response increased risk perception due to domestic or international
191 COVID-19-related reports. This finding may also suggest that severe NPIs, such as lockdowns,
192 were unnecessary, and that milder measures that were adopted by the population, possibly due to
193 government recommendations, media coverage, and social networks, could have been sufficient for
194 epidemic control. **check if this is true** Indeed, the evidence supports a change in transmission dynamics
195 (i.e. a model with τ) even for Sweden, in which a lockdown was not implemented⁵, suggesting that
196 lockdowns may not be necessary if other NPIs are adopted early enough during the outbreak (Sweden
197 banned public events on Mar 12, encouraged social distancing on Mar 16, and closed schools on
198 Mar 18⁵.)

199 We have found that the evidence supports a model in which the parameters change at a specific
200 time point τ over a model without such a change-point. It may be interesting to investigate if the
201 evidence favors a model with *two* change-points, rather than one. Two such change-points could reflect
202 escalating NPIs (e.g. school closures followed by lockdowns), a mix of NPIs and changes in weather,
203 a mix of domestic and international effects on risk perception, or other similar factors.

204 As several countries (e.g. Austria, Israel) begin to relieve lockdowns and ease restrictions, we expect
205 similar delays and advances to occur: in some countries people will begin to behave as if restrictions
206 were eased even before the official date, and in some countries people will continue to self-restrict
207 even after restrictions are officially removed. Such delays and advances could confuse analyses and
208 lead to wrong conclusions about the effects of NPI removals.

209 **Conclusions.** We have estimated the effective start date of NPIs and found that they often differ
210 from the official dates. Our results emphasize the complex interaction between personal, regional,
211 and global determinants of behavioral. Thus, our results highlight the need to further study variability
212 in compliance and behavior over both time and space. This can be accomplished both by surveying
213 differences in compliance within and between populations², and by incorporating specific behavioral
214 models into epidemiological models^{1,4}.

215 Acknowledgements

216 This work was supported in part by the Israel Science Foundation 552/19 and 1399/17.

- [1] Arthur, R. F., Jones, J. H., Bonds, M. H. and Feldman, M. W. 2020, 'Complex dynamics induced by delayed adaptive behavior during outbreaks', *bioRxiv* pp. 1–23.
- [2] Atchison, C. J., Bowman, L., Vrinten, C., Redd, R., Pristera, P., Eaton, J. W. and Ward, H. 2020, 'Perceptions and behavioural responses of the general public during the COVID-19 pandemic: A cross-sectional survey of UK Adults', *medRxiv* p. 2020.04.01.20050039.
- [3] Dunn, A. G., Leask, J., Zhou, X., Mandl, K. D. and Coiera, E. 2015, 'Associations between exposure to and expression of negative opinions about human papillomavirus vaccines on social media: An observational study', *J. Med. Internet Res.* **17**(6), e144.
- [4] Fenichela, E. P., Castillo-Chavez, C., Ceddiac, M. G., Chowell, G., Gonzalez Parrae, P. A., Hickling, G. J., Holloway, G., Horan, R., Morin, B., Perrings, C., Springborn, M., Velazquez, L. and Villalobos, C. 2011, 'Adaptive human behavior in epidemiological models', *Proc. Natl. Acad. Sci. U. S. A.* **108**(15), 6306–6311.
- [5] Flaxman, S., Mishra, S., Gandy, A., Unwin, J. T., Coupland, H., Mellan, T. A., Zhu, H., Berah, T., Eaton, J. W., Guzman, P. N. P., Schmit, N., Cilloni, L., Ainslie, K. E. C., Baguelin, M., Blake, I., Boonyasiri, A., Boyd, O., Cattarino, L., Ciavarella, C., Cooper, L., Cucunubá, Z., Cuomo-Dannenburg, G., Dighe, A., Djaafara, B., Dorigatti, I., Van Elsland, S., Fitzjohn, R., Fu, H., Gaythorpe, K., Geidelberg, L., Grassly, N., Green, W., Hallett, T., Hamlet, A., Hinsley, W., Jeffrey, B., Jorgensen, D., Knock, E., Laydon, D., Nedjati-Gilani, G., Nouvellet, P., Parag, K., Siveroni, I., Thompson, H., Verity, R., Volz, E., Gt Walker, P., Walters, C., Wang, H., Wang, Y., Watson, O., Xi, X., Winskill, P., Whittaker, C., Ghani, A., Donnelly, C. A., Riley, S., Okell, L. C., Vollmer, M. A. C., Ferguson, N. M. and Bhatt, S. 2020, 'Estimating the number of infections and the impact of non-pharmaceutical interventions on COVID-19 in 11 European countries', *Imp. Coll. London* (March), 1–35.
- [6] Foreman-Mackey, D., Hogg, D. W., Lang, D. and Goodman, J. 2013, 'emcee : The MCMC Hammer', *Publ. Astron. Soc. Pacific* **125**(925), 306–312.
- [7] Gatto, M., Bertuzzo, E., Mari, L., Miccoli, S., Carraro, L., Casagrandi, R. and Rinaldo, A. 2020, 'Spread and dynamics of the COVID-19 epidemic in Italy: Effects of emergency containment measures', *Proc. Natl. Acad. Sci.* p. 202004978.
- [8] Kaufman, M. R., Cornish, F., Zimmerman, R. S. and Johnson, B. T. 2014, 'Health behavior change models for HIV prevention and AIDS care: Practical recommendations for a multi-level approach', *J. Acquir. Immune Defic. Syndr.* **66**(SUPPL.3), 250–258.
- [9] Li, R., Pei, S., Chen, B., Song, Y., Zhang, T., Yang, W. and Shaman, J. 2020, 'Substantial undocumented infection facilitates the rapid dissemination of novel coronavirus (SARS-CoV2)', *Science* (80-). p. eabb3221.
- [10] Pei, S. and Shaman, J. 2020, 'Initial Simulation of SARS-CoV2 Spread and Intervention Effects in the Continental US', *medRxiv* p. 2020.03.21.20040303.
- [11] Spiegelhalter, D. J., Best, N. G., Carlin, B. P. and Van Der Linde, A. 2002, 'Bayesian measures of model complexity and fit', *J. R. Stat. Soc. Ser. B Stat. Methodol.* **64**(4), 583–616.
- [12] Wiyeh, A. B., Cooper, S., Nnaji, C. A. and Wiysonge, C. S. 2018, 'Vaccine hesitancy – Outbreaks': using epidemiological modeling of the spread of ideas to understand the effects of vaccine related events on vaccine hesitancy', *Expert Rev. Vaccines* **17**(12), 1063–1070.
- [13] Zipfel, C. M. and Bansal, S. 2020, 'Assessing the interactions between COVID-19 and influenza in the United States', *medRxiv* (February), 1–13.

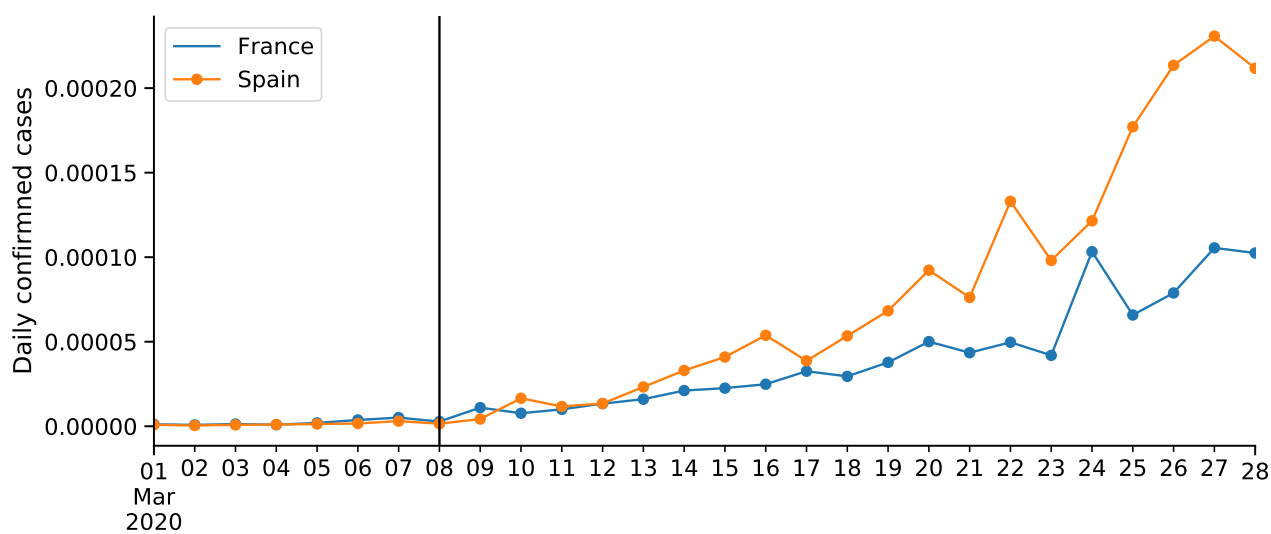


Figure S1: COVID-19 confirmed cases in France and Spain. Number of cases proportional to population size (as of 2018). Vertical line shows Mar 8, the effective start of NPIs \hat{t} in both countries.